# CONTROL OF GRAPH SIGNALS OVER RANDOM TIME-VARYING GRAPHS

*Fernando Gama*[†], *Elvin Isufi*[‡], *Geert Leus*[‡] *and Alejandro Ribeiro*[†]

† Department of Electrical and Systems Engineering, University of Pennsylvania, Philadelphia, PA
‡ Department of Microelectronics, Delft University of Technology, Delft, the Netherlands

## ABSTRACT

In this work, we jointly exploit tools from graph signal processing and control theory to drive a bandlimited graph signal that is being diffused on a random time-varying graph from a subset of nodes. As our main contribution, we rely *only on the statistics* of the graph to introduce the concept of *controllability in the mean*, and therefore drive the signal on the expected graph to a desired bandlimited state. A mean-square error (MSE) analysis is performed for two main tasks: $i)$ to highlight the role played by the signal bandwidth and the control nodes to the deviation from the mean signal of a particular realization; and $ii)$ to select the control nodes and design the control signal that minimize this MSE. Numerical results validate the introduced *controllability in the mean* framework and show its ability to cope with time-varying topologies.

***Index Terms—*** Graph signal processing, random graphs, time-varying graphs, control, complex networks.

## 1. INTRODUCTION

Graph signal processing (GSP) emerged recently as a novel framework to process signals defined on the vertices of a graph (i.e. graph signals) [1]. Examples of interest are load charge in smart grids, fMRI measurements on brain networks, and traffic monitoring on road networks. Differently from other network processing techniques, GSP introduces a spectral analysis on graphs [1, 2], which allows us to process graph signals in the so-called graph Fourier domain rather than only in the vertex domain. Motivated by this unique way of processing graph signals, several signal processing concepts such as filtering [2–6], sampling [7–10] and adaptive algorithms [11–13] have been extended in the GSP context.

Another interesting task that has found an extension to GSP is the control of a graph signal diffusion, i.e., driving a signal that is being diffused over the graph to a desired state. Specifically, [14, 15] have shown that this task can be achieved by acting only on a few relevant nodes, referred to as the control nodes. However, in applications including smart grids and road networks, the graph topology has more often a stochastic nature due to link or sensor failures, such as grid problems or street closure [16]. In this instance, the signal will be diffused on random graph realizations and, therefore, we should account for the graph randomness in controlling the diffusion.

In this work, we take one step further by extending the control of graph signals to a stochastic environment. Specifically, by considering the graph signal being diffused over a random edge sampling (RES) graph model [16, 17], we introduce the concept of *controllability in the mean*. This approach is blind to the specific realizations of the graph and accounts only for the graph statistics to drive the expected signal, i.e., the signal that is diffused on the expected graph, to a desired bandlimited state. In addition, to perform control from few nodes we consider the graph signal to be now bandlimited w.r.t. the expected graph, though this might not be the case for the particular realizations. An important consequence is that the controlled particular realization becomes a random variable, and thus it might deviate from the expected state. To quantify for this deviation, we perform a mean-square error (MSE) analysis that $i)$ highlights the role played by the different actors, such as the graph statistics, the signal bandwidth and the control nodes; and $ii)$ serves as a performance measure to jointly pick the control nodes and design the respective control signals such that a target MSE deviation from the expected state is guaranteed. To the best of our knowledge this is the first contribution that approaches sparse controllability of network signals from this statistical viewpoint.

Our results are validated by numerical simulations, which show the potential of the controllability in the mean approach to perform graph signal control on random time-varying graphs.

## 2. BACKGROUND

This section covers some background concepts that are exploited throughout the paper. Specifically, we review the basics of GSP, the considered RES graph model and diffusion control over time-invariant graphs.

**GSP basics.** Consider an undirected graph $\mathcal{G} = (\mathcal{V}, \mathcal{E}, \boldsymbol{W})$, with $\mathcal{V}$ the set of $N$ nodes (vertices), $\mathcal{E}$ the edge set, and $\boldsymbol{W}$ denoting the weighted adjacency matrix with $W_{n,m} = W_{m,n} > 0$ if the vertices $v_n$ and $v_m$ are connected (i.e., $(n, m) \in \mathcal{E}$) and $W_{n,m} = 0$, otherwise. A graph signal $\boldsymbol{x}$ is defined as a mapping from the vertex set to the field of complex numbers, i.e., $\boldsymbol{x} : \mathcal{V} \to \mathbb{C}$ with the $n$th entry $x_n$ representing the signal value on the node $v_n$. Next to $\boldsymbol{W}$, another matrix that captures the graph connectivity is the graph Laplacian matrix $\boldsymbol{L} = \text{diag}(\boldsymbol{1}_N^{\mathsf{T}}\boldsymbol{W}) - \boldsymbol{W}$ or any generalization of it (e.g., the normalized Laplacian matrix) [18]. Since $\boldsymbol{L}$ is real and symmetric it enjoys an eigendecomposition $\boldsymbol{L} = \boldsymbol{V}\boldsymbol{\Lambda}\boldsymbol{V}^{\mathsf{H}}$, where $\boldsymbol{V} = [\boldsymbol{v}_1, \ldots, \boldsymbol{v}_N]$ denotes the eigenvector matrix and $\boldsymbol{\Lambda} = \text{diag}(\lambda_1, \ldots, \lambda_N)$ contains the eigenvalues of $\boldsymbol{L}$. Throughout this work we consider graphs with Laplacians $\boldsymbol{L}$ belonging to some set $\mathcal{L}$ with finite spectral norm $\|\boldsymbol{L}\| \leq \varrho$.

The projection of $\boldsymbol{x}$ onto the eigenbasis $\boldsymbol{V}$ is defined as the graph Fourier transform (GFT) and is denoted as $\hat{\boldsymbol{x}} = \boldsymbol{V}^{\mathsf{H}}\boldsymbol{x}$ [1], where the $n$th entry $\hat{x}_n$ denotes the $n$th Fourier coefficient. Using this analogy, $\boldsymbol{v}_n$ is the $n$th frequency basis and $\lambda_n$ the $n$th graph frequency. Likewise, the graph signal $\boldsymbol{x}$ can be written as a linear combination of the frequency basis weighted by the frequency coefficients, $\boldsymbol{x} = \boldsymbol{V}\hat{\boldsymbol{x}}$, an operation known as the inverse GFT. A graph signal is said to be *bandlimited* if it has a sparse support in the graph frequency domain (i.e., it has few nonzero frequency coefficients). Without loss

Supported by NSF CCF 1717120 and ARO W911NF1710438. Email contact: {fgama,aribeiro}@seas.upenn.edu, {e.isufi-1,g.j.t.leus}@tudelft.nl.

of generality, assume that the first $K$ elements of $\hat{\boldsymbol{x}}$ are nonzero, so we can write $\hat{\boldsymbol{x}} = [\hat{\boldsymbol{x}}_K^\mathsf{T}, \mathbf{0}_{N-K}^\mathsf{T}]^\mathsf{T}$ where $\hat{\boldsymbol{x}}_K \in \mathbb{C}^K$ and $\mathbf{0}_{N-K}$ is the all-zero vector of length $N-K$. Then, by partitioning $\boldsymbol{V}$ as $\boldsymbol{V} = [\boldsymbol{V}_K, \boldsymbol{V}_{N-K}]$ a bandlimited graph signal can be expressed in the compact form $\boldsymbol{x} = \boldsymbol{V}_K \hat{\boldsymbol{x}}_K$ and similarly $\hat{\boldsymbol{x}}_K = \boldsymbol{V}_K^\mathsf{H} \boldsymbol{x}$.

**Random graph model.** From [16], a RES realization $\mathcal{G}_t$ of the original graph $\mathcal{G}$ at time $t$ is defined as:

**Definition 1** (RES graph model)**.** *In a RES realization $\mathcal{G}_t$ of an underlying graph $\mathcal{G}$ an edge $(m,n) \in \mathcal{E}$ is activated with a probability $0 < p_{m,n} \leq 1$. The edges are activated independently over both the graph and temporal dimension and are considered mutually independent from the graph signal if the latter has a stochastic nature.*

In other words, for each time instant $t$ we have a graph realization $\mathcal{G}_t = (\mathcal{V}, \mathcal{E}_t)$ drawn from the underlying graph $\mathcal{G} = (\mathcal{V}, \mathcal{E})$, where the edge set $\mathcal{E}_t \subseteq \mathcal{E}$ is generated via an independent Bernoulli process. For what regards this work, we consider $p_{n,m} = p_{\text{act}}$, i.e. all edges of the underlying graph to be activated with the same probability. Refer to $\boldsymbol{L}$ as the graph Laplacian relative to the graph $\mathcal{G}$ and to $\boldsymbol{L}_t$ as the graph Laplacian relative to the graph realization $\mathcal{G}_t$. To ease the exposition, let us further denote the expected Laplacian $\mathbb{E}[\boldsymbol{L}_t]$ as $\bar{\boldsymbol{L}}$ related to the expected graph $\bar{\mathcal{G}}$. Note that $\bar{\boldsymbol{L}} = p_{\text{act}} \boldsymbol{L}$, i.e., the expected Laplacian is a scaled version of the Laplacian matrix of the underlying graph $\mathcal{G}$. Since $\boldsymbol{L} \in \mathcal{L}$ and $\mathcal{E}_t \subseteq \mathcal{E}$, the instantaneous Laplacians $\boldsymbol{L}_t$ of $\mathcal{G}_t$ belong also to $\mathcal{L}$, meaning that all $\boldsymbol{L}_t$ have bounded eigenvalues. From the interlacing property [19], the following holds $\|\boldsymbol{L}_t\| \leq \|\boldsymbol{L}\| \leq \varrho$ for all $t$.

**Diffusion control over graphs.** With $\boldsymbol{x}(t)$ denoting the continuous-time graph signal at time $t$, its instantaneous diffusion follows the model $\partial \boldsymbol{x}/\partial t = -\boldsymbol{L}\boldsymbol{x}(t)$, which in a discretized form can be expressed as

$$\boldsymbol{x}_{t+1} = (\boldsymbol{I} - \epsilon \boldsymbol{L})\boldsymbol{x}_t := \boldsymbol{A}\boldsymbol{x}_t \tag{1}$$

where $\boldsymbol{A} = \boldsymbol{I} - \epsilon \boldsymbol{L}$ is commonly referred to as the state transition matrix. To guarantee the stability of (1), $\epsilon$ has to satisfy $0 < \epsilon \leq 1/\varrho$. Then, the steering of (1) from the initial graph signal $\boldsymbol{x}_0$ to a desired state $\boldsymbol{x}^*$ in $T$ steps amounts to designing the input signals $\boldsymbol{u}_t$ on the nodes $\mathcal{V}$ through the linear system

$$\boldsymbol{x}_{t+1} = \boldsymbol{A}\boldsymbol{x}_t + \boldsymbol{B}\boldsymbol{u}_t, \tag{2}$$

with $\boldsymbol{B}$ denoting the control input matrix. It is clear that system (2) is controllable if and only if the controllability matrix

$$\boldsymbol{C} = [\boldsymbol{B}, \boldsymbol{A}\boldsymbol{B}, \ldots, \boldsymbol{A}^{T-1}\boldsymbol{B}] \tag{3}$$

has full row rank, i.e., $\text{rank}(\boldsymbol{C}) = N$ [20]. The authors in [15] perform sparse control in a graph-time fashion by designing $\boldsymbol{u} = [\boldsymbol{u}_0, \ldots, \boldsymbol{u}_{T-1}]$ that minimizes the cost function $f(\boldsymbol{u}) = \|\boldsymbol{u}\|_2^2 + \gamma\|\boldsymbol{u}\|_0$ w.r.t. $\boldsymbol{u}$ such that $\boldsymbol{x}_T = \boldsymbol{x}^*$.

However, the control nodes are not fixed over time. Further, the impact of the signal bandwidth on the controlled signal $\boldsymbol{x}_T$, as well as the conditions that $\boldsymbol{B}$ should satisfy for $\boldsymbol{C}$ to be full rank remain still open problems. In the next section, we answer these questions and show that sparse control of graph signals can be directly performed in the graph Fourier domain. These aspects will then result useful also for the controllability in the mean approach of Section 4.

## 3. SPARSE CONTROL IN THE GRAPH FOURIER DOMAIN

In this section we formulate the framework of driving system (2) to a desired *bandlimited* state $\boldsymbol{x}^* = \boldsymbol{V}_K^\mathsf{H} \hat{\boldsymbol{x}}_K^*$ from a subset of nodes $\mathcal{S} \subseteq \mathcal{V}$ with a bandlimited control signal $\boldsymbol{u}_t = \boldsymbol{V}_K^\mathsf{H} \hat{\boldsymbol{u}}_{t,K}$. As bandlimited graph signals concentrate their energy in few Fourier coefficients, they facilitate follow-up tasks such as subsampling and denoising. We also remark that the design costs for the control signals is now significantly reduced, as the control matrix will have lower dimensions.

Then, by applying the GFT to (2) we have

$$\hat{\boldsymbol{x}}_{t+1} = \hat{\boldsymbol{A}}\hat{\boldsymbol{x}}_t + \boldsymbol{V}^\mathsf{H}\boldsymbol{B}\boldsymbol{u}_t, \tag{4}$$

where $\hat{\boldsymbol{A}} = \boldsymbol{V}^\mathsf{H}\boldsymbol{A}\boldsymbol{V}$. As in graph signal diffusion processes, $\boldsymbol{A}$ shares the eigenvectors of the graph Laplacian $\boldsymbol{L}$ [e.g., (1)], we have $\hat{\boldsymbol{A}} = \text{diag}(\hat{\boldsymbol{a}})$, with the vector $\hat{\boldsymbol{a}} \in \mathbb{C}^N$ containing the spectrum of the matrix $\boldsymbol{A}$. Furthermore, as our aim is to drive the graph signal from a subset of nodes, we consider $\boldsymbol{B}$ to be a diagonal selection matrix, i.e., $\boldsymbol{B} = \boldsymbol{D} := \text{diag}(\boldsymbol{d})$ such that $d_{n,n} = 1$ if the $v_n$th node is used for control and zero otherwise.

We can write (4) as

$$\begin{bmatrix} \hat{\boldsymbol{x}}_{t+1,K} \\ \hat{\boldsymbol{x}}_{t+1,N-K} \end{bmatrix} = \begin{bmatrix} \text{diag}(\hat{\boldsymbol{a}}_K)\hat{\boldsymbol{x}}_{t,K} \\ \text{diag}(\hat{\boldsymbol{a}}_{N-K})\hat{\boldsymbol{x}}_{t,N-K} \end{bmatrix} + \boldsymbol{V}^\mathsf{H}\boldsymbol{D}[\boldsymbol{V}_K, \boldsymbol{V}_{N-K}] \begin{bmatrix} \hat{\boldsymbol{u}}_{t,K} \\ \hat{\boldsymbol{u}}_{t,N-K} \end{bmatrix} \tag{5}$$

where $\text{diag}(\hat{\boldsymbol{a}}_K)$ and $\text{diag}(\hat{\boldsymbol{a}}_{N-K})$ are diagonal matrices containing respectively the first $K$ and the last $N-K$ elements of $\hat{\boldsymbol{a}}$ in the main diagonal; $\hat{\boldsymbol{u}}_{t,K}$ is the $K \times 1$ vector consisting of the first $K$ elements of the GFT of $\boldsymbol{u}_t$ and $\hat{\boldsymbol{u}}_{t,N-K}$ is a $(N-K) \times 1$ vector containing the remaining $N-K$ elements of $\hat{\boldsymbol{u}}_t$. Then, for control signals that are bandlimited w.r.t. the underlying graph (i.e., $\hat{\boldsymbol{u}}_{t,N-K} = \mathbf{0}_{N-K}$, for all $t \geq 0$), (5) becomes

$$\begin{bmatrix} \hat{\boldsymbol{x}}_{t+1,K} \\ \hat{\boldsymbol{x}}_{t+1,N-K} \end{bmatrix} = \begin{bmatrix} \text{diag}(\hat{\boldsymbol{a}}_K)\hat{\boldsymbol{x}}_{t,K} \\ \text{diag}(\hat{\boldsymbol{a}}_{N-K})\hat{\boldsymbol{x}}_{t,N-K} \end{bmatrix} + \boldsymbol{V}^\mathsf{H}\boldsymbol{D}\boldsymbol{V}_K\hat{\boldsymbol{u}}_{t,K}. \tag{6}$$

Recursion (6) leads to two main observations: $i$) under the condition that the tuple $(\hat{\boldsymbol{A}}, \boldsymbol{V}^\mathsf{H}\boldsymbol{D}\boldsymbol{V}_K)$ is controllable, we can drive $\boldsymbol{x}_t$ to any desired signal $\boldsymbol{x}^*$ with a bandlimited input signal $\hat{\boldsymbol{u}}_{t,K}$; and $ii$) the selection constraint on the control signals implies that it is not possible to keep the system evolving within the subspace of bandlimited graph signals. However, the latter is not a big issue as we can still focus on controlling $\boldsymbol{x}_T$ to a desired bandlimited frequency content $\hat{\boldsymbol{x}}_K^*$, and then filter out the spurious high-pass frequency content of $\boldsymbol{x}_T$ to obtain the desired signal in the vertex domain $\boldsymbol{x}^* = \boldsymbol{V}_K\hat{\boldsymbol{x}}_K^*$. In other words, by denoting $\hat{\boldsymbol{A}}_K = \text{diag}(\hat{\boldsymbol{a}}_K)$ we only focus on the dynamics of the first $K$ Fourier coefficients [cf. (6)]

$$\hat{\boldsymbol{x}}_{t+1,K} = \hat{\boldsymbol{A}}_K\hat{\boldsymbol{x}}_{t,K} + \boldsymbol{V}_K^\mathsf{H}\boldsymbol{D}\boldsymbol{V}_K\hat{\boldsymbol{u}}_{t,K} \tag{7}$$

to obtain a graph signal $\boldsymbol{x}_T$ such that $\hat{\boldsymbol{x}}_{T,K} = \hat{\boldsymbol{x}}_K^*$, and then we use a low-pass filter $\boldsymbol{H}_{\text{LP}} = \boldsymbol{V}_K\boldsymbol{V}^\mathsf{H}$ that results in the controlled bandlimited signal $\boldsymbol{x}_T^* = \boldsymbol{H}_{\text{LP}}\boldsymbol{x}_T$. The design variables in our case are the sampling matrix $\boldsymbol{D}$ that selects $M \leq N$ control nodes and the bandlimited control signals $\hat{\boldsymbol{u}}_t \in \mathbb{R}^N$ for all $t = 0, \ldots, T-1$. With this in place, we claim our first contribution.

**Proposition 1.** *Let $\boldsymbol{x}_t$ be a graph signal that is being diffused over an $N$-node graph $\mathcal{G}$ with graph Laplacian $\boldsymbol{L} = \boldsymbol{V}\boldsymbol{\Lambda}\boldsymbol{V}^\mathsf{H}$. Let also $\{\boldsymbol{u}_t\}_{t=0}^{T-1} = \{\boldsymbol{V}_k^\mathsf{H}\hat{\boldsymbol{u}}_{t,K}\}_{t=0}^{T-1}$ denote a sequence of bandlimited control signals acting on $M \leq N$ nodes as in* (7) *. Then, a necessary condition to drive $\boldsymbol{x}_t$ to a desired bandlimited state $\boldsymbol{x}^* = \boldsymbol{V}_K\hat{\boldsymbol{x}}^*$ in the graph Fourier domain [cf.* (7)*] is that at least $M \geq K/T$ nodes must be selected to inject the input signal into the system.*

*Proof.* System (7) is controllable if and only if the matrix $\hat{\boldsymbol{C}} = [\hat{\boldsymbol{B}}_K, \hat{\boldsymbol{A}}_K\hat{\boldsymbol{B}}_K, \ldots, \hat{\boldsymbol{A}}_K^{T-1}\hat{\boldsymbol{B}}_K]$ has full row rank, where $\hat{\boldsymbol{B}}_K = \boldsymbol{V}_K^{\mathsf{H}}\boldsymbol{D}\boldsymbol{V}_K$. Differently, we can write $\hat{\boldsymbol{C}}$ as

$$\hat{\boldsymbol{C}} = \left[\boldsymbol{I}_K, \hat{\boldsymbol{A}}_K, \hat{\boldsymbol{A}}_K^2, \ldots, \hat{\boldsymbol{A}}_K^{T-1}\right](\boldsymbol{I}_T \otimes \hat{\boldsymbol{B}}_K), \tag{8}$$

with $\otimes$ denoting the Kronecker product. From (8) we note that $\text{rank}(\hat{\boldsymbol{C}})$ depends on the rank of the $TK \times TN$ matrix $(\boldsymbol{I}_T \otimes \boldsymbol{V}_K^{\mathsf{H}}\boldsymbol{D}\boldsymbol{V}_K)$ as the other term has full rank $K$. Then, as $\text{rank}(\boldsymbol{I}_T \otimes \boldsymbol{V}_K^{\mathsf{H}}\boldsymbol{D}\boldsymbol{V}_K) = T\text{rank}(\boldsymbol{V}_K^{\mathsf{H}}\boldsymbol{D}\boldsymbol{V}_K) \leq T\min\{K, M\}$, we have that $\hat{\boldsymbol{C}}$ has full rank only if $TM \geq K$. This concludes the proof. □

We remark that Proposition 1 only provides a necessary condition on the minimum number of nodes required to control a graph signal from the graph spectral domain. Thus, in practice the controllability performance is affected by the number of control nodes $M$ as $\hat{\boldsymbol{C}}$ may easily lose rank depending on the selected control nodes. In addition, as mentioned at the end of Section 2, differently from prior art, the proposed framework highlights the role played by the graph topology (through the dependence of (8) on $\boldsymbol{V}_K$), the graph signal bandwidth and the control nodes on the control matrix. Finally, we remark that the tradeoff given by the necessary condition $M \geq K/T$ between the number of control nodes $M$ and the time horizon is reminiscent of the tradeoff studied in [14] for graph signal reconstruction through percolation.

## 4. CONTROLLABILITY IN THE MEAN

We now consider the case where the underlying topology changes over time according to the RES graph model (Def. 1). The objective is to drive the system to a desired bandlimited graph signal *in the mean* over a finite time horizon $T$. This is to be achieved by designing the control signals $\{\hat{\boldsymbol{u}}_{\tau,K}\}_{\tau=0}^{T-1}$ to be applied at the $M$ control nodes following the dynamics of system (7). In this instance, the bandlimitedness of the signals is considered w.r.t. the expected graph. We remark that for a particular $\mathcal{G}_t$ the signal on the vertex domain might not be bandlimited. To quantify the performance, we provide a mean square analysis that highlights the distance between a particular controlled realization and the expected controlled signal.

**Mean controllability.** For a time-varying graph, we write the dynamical system (2) as

$$\boldsymbol{x}_{t+1} = \boldsymbol{A}_t\boldsymbol{x}_t + \boldsymbol{B}\boldsymbol{u}_t, \tag{9}$$

where $\boldsymbol{A}_t = \boldsymbol{I} - \epsilon\boldsymbol{L}_t$ accounts for the RES graph variations $\mathcal{G}_t$. By applying the expectation operator to (2) we have

$$\begin{aligned}\boldsymbol{\mu}_{t+1} &= \mathbb{E}[\boldsymbol{x}_{t+1}] = \mathbb{E}[\boldsymbol{A}_t]\mathbb{E}[\boldsymbol{x}_t] + \boldsymbol{B}\boldsymbol{u}_t \\ &= \bar{\boldsymbol{A}}\boldsymbol{\mu}_t + \boldsymbol{B}\boldsymbol{u}_t,\end{aligned} \tag{10}$$

where in (10): $i)$ we exploited the fact that the RES graph realization at time $t$, $\boldsymbol{A}_t$, is independent from all past history of the signal evolution $\{\boldsymbol{x}_\tau\}_{\tau=0}^{t-1}$; and $ii)$ $\bar{\boldsymbol{A}} = \boldsymbol{I} - \epsilon\bar{\boldsymbol{L}} = \boldsymbol{I} - \epsilon p_{\text{act}}\boldsymbol{L}$. Then, from Sylvester's matrix theorem $\bar{\boldsymbol{A}}$ has the eigendecomposition $\bar{\boldsymbol{A}} = \boldsymbol{V}(\boldsymbol{I} - \epsilon p_{\text{act}}\boldsymbol{\Lambda})\boldsymbol{V}^{\mathsf{H}} = \boldsymbol{V}\text{diag}(\bar{\boldsymbol{a}})\boldsymbol{V}^{\mathsf{H}}$, i.e., it shares the same eigenvectors of the underlying graph Laplacian $\boldsymbol{L}$ and its eigenvalues are $\text{diag}(\bar{\boldsymbol{a}}) = (\boldsymbol{I} - \epsilon p_{\text{act}}\boldsymbol{\Lambda})$.

Note that the *mean* evolution (10) is a deterministic system analogous to (2). Therefore, by proceeding in the same way as in Section 3 we can drive the bandlimited mean signal to a desired state $\hat{\boldsymbol{\mu}}_{T,K} = \hat{\boldsymbol{\mu}}_K^*$ through a sequence of deterministic bandlimited control signals $\{\hat{\boldsymbol{u}}_{\tau,K}\}_{\tau=0}^{T-1}$. Once again, the bandlimtedness is now w.r.t. the expected graph $\bar{\mathcal{G}}$, which for the considered case turns out to be a scaled version of the underlying graph $\mathcal{G}$. Then, we can write the equivalent of (7) for the mean evolution as

$$\hat{\boldsymbol{\mu}}_{t+1,K} = \text{diag}(\bar{\boldsymbol{a}}_K)\hat{\boldsymbol{\mu}}_{t,K} + \boldsymbol{V}_K^{\mathsf{H}}\boldsymbol{D}\boldsymbol{V}_K\hat{\boldsymbol{u}}_{t,K}, \tag{11}$$

which can be then used to obtain the mean signal $\boldsymbol{\mu}_T$ such that $\hat{\boldsymbol{\mu}}_{T,K} = \hat{\boldsymbol{\mu}}_K^*$. Finally, $\boldsymbol{\mu}_T$ is filtered by the (deterministic) low-pass filter $\boldsymbol{H}_{\text{LP}}$ to obtain the desired control signal $\boldsymbol{\mu}^* = \boldsymbol{H}_{\text{LP}}\boldsymbol{\mu}_T$.

**Mean square analysis.** Using (11) we can deterministically design the control signals $\{\hat{\boldsymbol{u}}_{\tau,K}\}_{\tau=0}^{T-1}$ and the choice of nodes to act upon so that the mean signal over the mean graph $\bar{\mathcal{G}}$ can be controlled. However, the actual signal is controlled over a realization of the graph $\mathcal{G}_t$. Therefore, it becomes of utmost importance to study the MSE of such an approach in order to assess its ability to actually control the signal. In what follows, we obtain a bound on the MSE that would later serve in the design of control strategies.

**Proposition 2.** *Let $\{\mathcal{G}_t, t \geq 0\}$ be a collection of graph realizations following the RES model (Def. 1) w.r.t. the underlying graph $\mathcal{G}$. Let $\varrho > 0$ be the bound on the spectral norm of this collection. Assume that we control the signal with $\boldsymbol{x}_0 = \boldsymbol{0}$ and let $\boldsymbol{\mu}_T = \boldsymbol{\mu}^*$ be the desired mean signal, then*

$$\mathbb{E}\left[\|\boldsymbol{x}_T - \boldsymbol{\mu}_T\|_2^2\right] \leq \sum_{\tau=0}^{T-1}\sum_{\tau'=0}^{T-1} \text{tr}\left[\boldsymbol{B}\boldsymbol{u}_\tau\boldsymbol{u}_{\tau'}^{\mathsf{H}}\boldsymbol{B}^{\mathsf{H}}\right] \tag{12}$$

*Proof.* At any given time $t$, the state of the system (9) can be written as

$$\boldsymbol{x}_t = \sum_{\tau=0}^{t-1}\boldsymbol{\Phi}_{t-1,\tau+1}\boldsymbol{B}\boldsymbol{u}_\tau, \tag{13}$$

where $\boldsymbol{\Phi}_{b,a} = \boldsymbol{A}_b\boldsymbol{A}_{b-1}\cdots\boldsymbol{A}_{a+1}\boldsymbol{A}_a$ for $b \geq a$ and $\boldsymbol{\Phi}_{b,a} = \boldsymbol{I}_N$ otherwise. Observe that (13) is similar to a FIR filter under stochasticity [16, Prop. 3]. Therefore, recalling that $\mathbb{E}[\|\boldsymbol{x}_t - \boldsymbol{\mu}_t\|_2^2] \leq \mathbb{E}[\text{tr}[\boldsymbol{x}_t\boldsymbol{x}_t^{\mathsf{H}}]]$ we obtain

$$\mathbb{E}\left[\text{tr}[\boldsymbol{x}_t\boldsymbol{x}_t^{\mathsf{H}}]\right] = \sum_{\tau=0}^{t-1}\sum_{\tau'=0}^{t-1}\mathbb{E}\left[\text{tr}[\boldsymbol{\Gamma}_{t-1}(\tau,\tau')]\right],$$

with $\boldsymbol{\Gamma}_{t-1}(\tau,\tau') = \boldsymbol{\Phi}_{t-1,\tau+1}\boldsymbol{B}\boldsymbol{u}_\tau\boldsymbol{u}_{\tau'}^{\mathsf{H}}\boldsymbol{B}^{\mathsf{H}}\boldsymbol{\Phi}_{t-1,\tau'+1}^{\mathsf{H}} \in \mathbb{R}^{N\times N}$. Using the inequality $\text{tr}[\boldsymbol{U}\boldsymbol{V}] \leq \|\boldsymbol{U}\|\text{tr}[\boldsymbol{V}]$ valid for any square matrix $\boldsymbol{U}$ and any positive semidefinite matrix $\boldsymbol{V}$ [21], together with submultiplicativity of the spectral norm, $\|\boldsymbol{U}\boldsymbol{V}\| \leq \|\boldsymbol{U}\|\|\boldsymbol{V}\|$, we get

$$\mathbb{E}\left[\text{tr}[\boldsymbol{\Gamma}_{t-1}(\tau,\tau')]\right] \leq \text{tr}\left[\boldsymbol{B}\boldsymbol{u}_\tau\boldsymbol{u}_{\tau'}^{\mathsf{H}}\boldsymbol{B}^{\mathsf{H}}\right]\mathbb{E}\left[\|\boldsymbol{\Phi}_{t-1,\tau'+1}^{\mathsf{H}}\|\|\boldsymbol{\Phi}_{t-1,\tau+1}\|\right].$$

Then, we bound the spectral norm of $\boldsymbol{A}_t = \boldsymbol{I} - \epsilon\boldsymbol{L}_t$ as $\|\boldsymbol{A}_t\| = \|\boldsymbol{I} - \epsilon\boldsymbol{L}_t\| = 1 - \epsilon\|\boldsymbol{L}_t\| \leq 1$. Therefore, using once again the submultiplicativity of the norms, we also bound $\|\boldsymbol{\Phi}_{t-1,\tau}\| \leq \prod_{t'=\tau+1}^{t-1}\|\boldsymbol{A}_{t-t'}\| \leq 1$ so that

$$\mathbb{E}\left[\text{tr}[\boldsymbol{\Gamma}_{t-1}(\tau,\tau')]\right] \leq \text{tr}\left[\boldsymbol{B}\boldsymbol{u}_\tau\boldsymbol{u}_{\tau'}^{\mathsf{H}}\boldsymbol{B}^{\mathsf{H}}\right].$$

Finally, replacing back this last inequality and evaluating at $t = T$ completes the proof. □

As we are interested in designing bandlimited control signals on few nodes, the following corollary relates the results of Proposition 2 to the signal bandwidth and control nodes.

**Corollary 1.** *Under the assumptions of Proposition 2 we have that*

$$\mathbb{E}\left[\|\boldsymbol{x}_T - \boldsymbol{\mu}_T\|_2^2\right] \leq \|\boldsymbol{V}_K^{\mathsf{H}}\text{diag}(\boldsymbol{d})\boldsymbol{V}_K\| \cdot \boldsymbol{1}_T^{\mathsf{T}}\boldsymbol{U}_K^{\mathsf{H}}\boldsymbol{U}_K\boldsymbol{1}_T \tag{14}$$

*where $\boldsymbol{U}_K = [\hat{\boldsymbol{u}}_{0,K}, \ldots, \hat{\boldsymbol{u}}_{T-1,K}] \in \mathbb{C}^{K\times T}$ and $\boldsymbol{1}_T$ is the all-one vector of size $T$.*

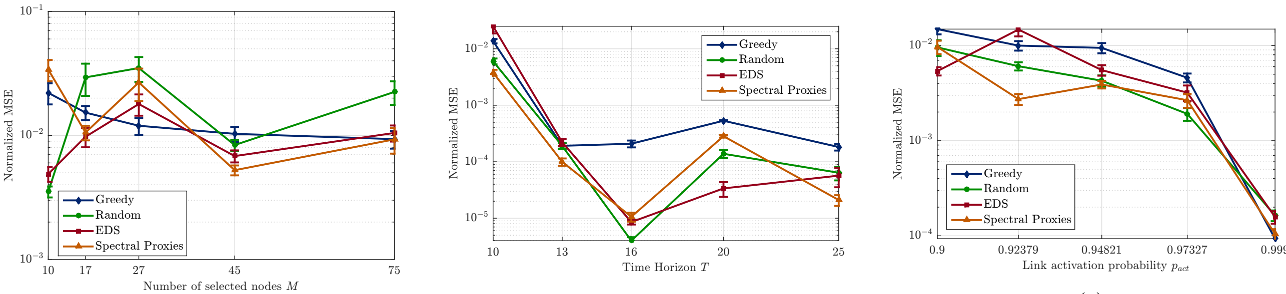


(a) (b) (c)

**Fig. 1**: NMSE averaged across 10 graphs and 100 RES realizations per graph. The error bars correspond to $1/8$ of the estimated variance. (a) Nodes selected $M$. There is a general drop in NMSE, especially for the greedy approach. (b) Time horizon $T$. The performance improves for larger $T$ and after $T = 13$ it drops below $10^{-3}$. (c) Activation probability $p_{\text{act}}$. It is noted that all MSE improves as $p_{\text{act}}$ tends to 1.

*Proof.* (Sketch) The claim can be proven by substituting $\boldsymbol{u}_\tau = \boldsymbol{V}_K \hat{\boldsymbol{u}}_{\tau,K}$ and $\boldsymbol{B} = \text{diag}(\boldsymbol{d})$ into (12) and then using the idempotence of $\text{diag}(\boldsymbol{d})$ together with the inequality $\text{tr}[\boldsymbol{U}\boldsymbol{V}] \leq \|\boldsymbol{U}\|\text{tr}[\boldsymbol{V}]$. □

We observe that the first term of the bound (14) highlights the importance of the tuple *signal bandwidth-graph topology* through $\boldsymbol{V}_K$ and that of the control nodes w.r.t. the underlying graph. The second term of (14), on the other hand, shows the role played by the control signals, all modulated by the graph spectrum. In the sequel, we show that bound (14) can be used to design optimal strategies that aim bounding the MSE to a desired value. We finally remark that the role of the graph statistics is overshadowed by the bound (14), but is highlighted in the mean controlled signal (11).

**Control strategy.** We postulate that the optimal control strategy is to jointly design $\boldsymbol{d}$ and $\{\hat{\boldsymbol{u}}_{\tau,K}\}_{\tau=0}^{T-1}$ such that the MSE bound (14) is minimized, subject to achieving an unbiased estimate at time horizon $T$ from $M$ control nodes. Specifically, the latter writes as

$$\underset{\substack{\boldsymbol{d}\in\{0,1\}^N \\ \boldsymbol{U}_K\in\mathbb{R}^{K\times T}}}{\text{minimize}} \quad \|\boldsymbol{V}_K^{\mathsf{H}}\text{diag}(\boldsymbol{d})\boldsymbol{V}_K\| \cdot \boldsymbol{1}_T^{\mathsf{T}}\boldsymbol{U}_K^{\mathsf{H}}\boldsymbol{U}_K\boldsymbol{1}_T \tag{15}$$

$$\text{subject to} \quad \boldsymbol{d}^{\mathsf{T}}\boldsymbol{1} = M,$$

$$\sum_{\tau=0}^{T-1}(\boldsymbol{I} - \epsilon p_{\text{act}}\boldsymbol{L})^{T-1-\tau}\text{diag}(\boldsymbol{d})\boldsymbol{V}_K\hat{\boldsymbol{u}}_{\tau,K} = \boldsymbol{\mu}_T.$$

Note that, while the objective function is not convex in $(\boldsymbol{d}, \{\hat{\boldsymbol{u}}_{\tau,K}\}_{\tau=0}^{T-1})$, it is convex in each of the design variables individually, regarding the other as fixed. We then approach (15) with a *suboptimal solution*, that first selects the control nodes such that (8) results in a full rank control matrix, and then design the control signals $\boldsymbol{U}_K$. Yet, even in the case of the proposed suboptimal solution, the problem remains non-convex due to the binary nature of the variable $\boldsymbol{d}$. We thus propose to greedily select the $M$ nodes, out of all the sets of nodes that lead to a full rank control matrix in (8), that minimize $\|\boldsymbol{V}_K^{\mathsf{H}}\text{diag}(\boldsymbol{d})\boldsymbol{V}_K\|$. Then, we solve the optimization problem (15) only for control signals $\boldsymbol{U}_K$ (which is now convex). In those cases where unbiasedness constraint renders the problem infeasible, we can relax this constraint to a small, tuned bias $\delta$ such that $\|\mathbb{E}[\boldsymbol{x}_T] - \boldsymbol{\mu}_T\| \leq \delta$.

## 5. NUMERICAL RESULTS

**Setup.** We consider a stochastic block model graph $\mathcal{G}$ of $N = 300$ nodes divided in four communities of 75 nodes each. The probability of edges within the same community is 0.9 while external edges are drawn with probability 0.4. We want to drive the system to a bandlimited signal $\hat{\boldsymbol{\mu}}_{T,K} = \boldsymbol{1}_K$ with $K = 10$, using $M$ nodes in a time horizon $T$ and where the RES model has activation probability $p_{m,n} = p_{\text{act}}$ for all edges. We consider four strategies to select nodes: $(i)$ the proposed greedy minimization of $\|\boldsymbol{V}_K^{\mathsf{H}}\text{diag}(\boldsymbol{d})\boldsymbol{V}_K\|$, $(ii)$ random node selection, $(iii)$ the experimental design (EDS) of [22], and $(iv)$ the spectral proxies method of [23]. We measure the performance in terms of normalized MSE (NMSE), w.r.t. the the controlled mean signal $\hat{\boldsymbol{\mu}}_T$. Our results are averaged over 10 different graphs realizations $\mathcal{G}$, where for each of them 100 RES realizations $\mathcal{G}_t$ are considered. The average NMSE and its variance are shown in Fig 1.

**Experiments.** First, we run simulations for varying number of selected nodes $M$, with $T = 10$ and $p_{\text{act}} = 0.9$. From the results in Fig. 1a, we see that the NMSE generally drops as more nodes are controlled. This is especially the case of the greedy approach. Second, in Fig. 1b, we fixed $M = 50$ and $p_{\text{act}} = 0.95$ and run tests for varying time horizon $T$. We observe that the NMSE lowers for increasing $T$ and for $T \geq 13$ the NMSE drops below $10^{-3}$ as the network has more time to contrast the link losses. Finally, we fix $M = 50$ and $T = 10$ and change the activation probability. The results in Fig. 1c show that the performance improves as $p_{\text{act}}$ tends to 1, since the realizations are more similar to the underlying graph for which the control strategy was designed. In general, we do not observe significant differences between the selection methods used, although the spectral proxies approach works slightly better.

## 6. CONCLUSIONS

This work proposed controllability of signals that are being diffused over random time-varying graphs. By simply relying on the statistics of the graph, we introduced the concept of observability in the mean to drive the graph signal to a desired state w.r.t. the expected graph. As most of the graph signals of interest are bandlimited w.r.t. the underlying graph, we rephrase the problem in the graph frequency domain to $i)$ select a fixed subset of nodes for control and $ii)$ design bandlimited control signals. We derive an upper bound on the MSE performance of the controlled signal and propose a controllability strategy that minimizes the MSE for a fixed number of control nodes. Numerical results show that an NMSE below $10^{-3}$ can be achieved, showing that the proposed controllability in the mean approach is effective in driving the system to a bandlimited state in presence of random link failures.

## 7. REFERENCES


[1] D. I Shuman, S. K. Narang, P. Frossard, A. Ortega, and P. Vandergheynst, "The emerging field of signal processing on graphs: Extending high-dimensional data analysis to networks and other irregular domains," *IEEE Signal Process. Mag.*, vol. 30, no. 3, pp. 83–98, May 2013.

[2] A. Sandryhaila and J. M. F. Moura, "Discrete signal processing on graphs," *IEEE Trans. Signal Process.*, vol. 61, no. 7, pp. 1644–1656, Apr. 2013.

[3] D. I. Shuman, P. Vandergheynst, D. Kressner, and P. Frossard, "Distributed signal processing via chebyshev polynomial approximation," *arXiv:1111.5239v3 [cs.DC]*, 29 July 2017.

[4] S. Segarra, A. G. Marques, and A. Ribeiro, "Optimal graph-filter design and applications to distributed linear network operators," *IEEE Trans. Signal Process.*, vol. 65, no. 15, pp. 4117–4131, Aug. 2017.

[5] E. Isufi, A. Loukas, A. Simonetto, and G. Leus, "Autoregressive moving average graph filtering," *IEEE Trans. Signal Process.*, vol. 65, no. 2, pp. 274–288, Jan. 2017.

[6] M. Coutino, E. Isufi, and G. Leus, "Distributed edge-variant graph filters," in *IEEE Int. Workshop Comput. Advances Multi-Sensor Adaptive Process. 2017*, Curaçao, Dutch Antilles, 10-13 Dec. 2017, IEEE.

[7] M. Tsitsvero, S. Barbarossa, and P. Di Lorenzo, "Signals on graphs: Uncertainty principle and sampling," *IEEE Trans. Signal Process.*, vol. 64, no. 18, pp. 4845–4860, Sep. 2016.

[8] S. Chen, R. Varma, A. Sandryhaila, and J. Kovacević, "Discrete signal processing on graphs: Sampling theory," *IEEE Trans. Signal Process.*, vol. 63, no. 24, pp. 6510–6523, Dec. 2015.

[9] A. G. Marques, S. Segarra, G. Leus, and A. Ribeiro, "Sampling of graph signals with successive local aggregations," *IEEE Trans. Signal Process.*, vol. 64, no. 7, pp. 1832–1843, Apr. 2016.

[10] F. Gama, A. G. Marques, G. Mateos, and A. Ribeiro, "Rethinking sketching as sampling: A graph signal processing approach," *arXiv:1611.00119v1 [cs.IT]*, 1 Nov. 2016.

[11] P. Di Lorenzo, S. Barbarossa, P. Banelli, and S. Sardellitti, "Adaptive least mean squares estimation of graph signals," *IEEE Trans. Signal, Inform. Process. Networks*, vol. 2, no. 4, pp. 555–568, Dec. 2016.

[12] P. Di Lorenzo, P. Banelli, E. Isufi, S. Barbarossa, and G. Leus, "Adaptive graph signal processing: Algorithms and optimal sampling strategies," *arXiv:1709.03726v1 [cs.LG]*, 12 Sep. 2017.

[13] P. Di Lorenzo, E. Isufi, P. Banelli, S. Barbarossa, and G. Leus, "Distributed recursive least squares strategies for adaptive reconstruction of graph signals," in *2017 25th Eur. Signal Process. Conf.*, Kos Island, Greece, 28 Aug.-2 Sep. 2017, Eur. Assoc. Signal Process.

[14] S. Segarra, A. G. Marques, G. Leus, and A. Ribeiro, "Reconstruction of Graph Signals Through Percolation from Seeding Nodes," *IEEE Trans. Signal Process.*, vol. 64, no. 16, pp. 4363–4378, Aug. 2016.

[15] S. Barbarossa, S. Sardellitti, and A. Farina, "On Sparse Controllability of Graph Signals," in *41st IEEE Int. Conf. Acoust., Speech and Signal Process.*, Shanghai, China, 20-25 March 2016, IEEE.

[16] E. Isufi, A. Loukas, A. Simonetto, and G. Leus, "Filtering random graph processes over random time-varying graphs," *IEEE Trans. Signal Process.*, vol. 65, no. 16, pp. 4406–4421, 18 May 2017.

[17] E. Isufi and G. Leus, "Distributed sparsified graph filters for denoising and diffusion tasks," in *42nd IEEE Int. Conf. Acoust., Speech and Signal Process.*, New Orleans, LA, 5-9 March 2017, IEEE.

[18] F. R. K. Chung, *Spectral Graph Theory*, Number 92 in Regional Conf. Series Math. Amer. Math. Soc., Providence, RI, 1997.

[19] G. Chen, G. Davis, F. Hall, Z. Li, K. Patel, and M. Stewart, "An interlacing result on normalized laplacians," *SIAM J. Discrete Math.*, vol. 18, no. 2, pp. 353–361, Aug. 2016.

[20] T. Kailath, *Linear Systems*, Prentice-Hall Inform. Syst. Sci. Series. Prentice-Hall, Englewood Cliffs, NJ, 1980.

[21] S.-D. Wang, T.-S. Kuo, and C.-F. Hsu, "Trace bounds on the solution of the algebraic matrix Riccati and Lyapunov equation," *IEEE Trans. Autom. Control*, vol. 31, no. 7, pp. 654–656, July 1986.

[22] R. Varma, S. Chen, and J. Kovacević, "Spectrum-blind signal recovery on graphs," in *2015 IEEE Int. Workshop Comput. Advances Multi-Sensor Adaptive Process.*, Cancún, México, 13-16 Dec. 2015, pp. 81–84, IEEE.

[23] A. Anis, A. Gadde, and A. Ortega, "Efficient sampling set selection for bandlimited graph signals using graph spectral proxies," *IEEE Trans. Signal Process.*, vol. 64, no. 14, pp. 3775–3789, July 2016.